The semiconductor-metal transition in fluid selenium studied by first-principles molecular-dynamics simulation

1998 J. Phys.: Condens. Matter 10 11429

(http://iopscience.iop.org/0953-8984/10/49/029)

J. Phys.: Condens. Matter **10** (1998) 11429–11438. Printed in the UK PII: S0953-8984(98)97985-1

The semiconductor–metal transition in fluid selenium studied by first-principles molecular-dynamics simulation

Kozo Hoshino and Fuyuki Shimojo

Faculty of Integrated Arts and Sciences, Hiroshima University, Higashi-Hiroshima 739-8521, Japan

Received 31 May 1998

Abstract. The changes in the structure and the electronic states of liquid selenium due to the semiconductor–metal (SC–M) transition at high temperatures and pressures are investigated by first-principles molecular-dynamics simulation using generalized-gradient-corrected density functional theory. It is found that the chain structure persists even in the metallic state, though the average length of the chains is decreasing with increasing temperature. From the time changes of the chain structure, it is also found that the interaction between the Se chains is crucially important for bond breaking, and that the bond breaking and the rearrangement of the Se chains occur more frequently at higher temperatures. When the Se–Se bonds break, the anti-bonding states above the Fermi level (E_F) are stabilized while the non-bonding states below E_F become unstable, and as a result the gap disappears at high temperatures. The eigenstates which fill up the energy gap and give rise to the metallic state of liquid Se have large amplitudes of wavefunctions near the ends of the Se chains.

To understand the experimentally observed photo-induced SC–M transition of liquid Se near the triple point, the possibility of inducing bond breaking in a Se chain by exciting an electron in the HOMO (highest occupied molecular orbital) to the LUMO (lowest unoccupied molecular orbital) is investigated by first-principles molecular-dynamics simulation and such a bond breaking is confirmed.

1. Introduction

Liquid selenium near its triple point is an assembly of helical chains of atoms with twofold coordination, and exhibits semiconducting behaviour. The average number of atoms per chain is estimated to be about 10^5 [1, 2] near the triple point and, with increasing temperature and pressure, it decreases rapidly and is estimated to be about 10 atoms near the critical point [3]. Accompanying this structural change, there is an increase in the electrical conductivity [4, 5] and the semiconductor–metal (SC–M) transition occurs at pressure $\geqslant$1 kbar near the critical point.

To investigate the relation of the SC–M transition to the structural change of liquid Se, Tamura and co-workers [7–9] carried out x-ray diffraction measurements for fluid Se up to the supercritical region, including the SC–M transition region. It was found that the twofold-coordinated structure is largely preserved even in the metallic region, and that the nearest-neighbour distance decreases slightly, this decrease being accompanied with the SC–M transition.

The SC–M transition in fluid Se has the following two characteristic features [8]:

(i) the electrical conductivity increases with decreasing density, which is contrary to the usual case; and

0953-8984/98/4911429+10$19.50

(ii) the metallic states appear when the average chain length becomes very short, which indicates that the SC–M transition is closely related to the instability of the chain structure [3, 8, 10].

Though there have been several theoretical studies for liquid Se using first-principles molecular-dynamics (MD) simulation [11–13], classical MD simulation [14] and Monte Carlo simulation [15], those studies are limited to the thermodynamic states near the triple point and along the liquid–vapour coexistence curve. Recently Shimojo *et al* [16] investigated the microscopic mechanism of the SC–M transition at high temperatures and pressures mentioned above using first-principles MD simulation. It was found that, at high temperatures, bond breaking and rearrangement of Se chains occur frequently due to the interchain interaction and that, when the bonds break, the anti-bonding states above the Fermi level are stabilized while the non-bonding (lone-pair) states below the Fermi level become unstable, and therefore the gap at the Fermi level disappears at high temperatures.

Quite recently, Sakaguchi and Tamura [17] measured the transient absorption spectra of liquid Se after illuminating it with a pulsed laser, and found that a giant photodarkening occurs and the optical gap disappears when the liquid Se is illuminated by a pulsed laser with the intensity of 15 mJ/pulse at 350 °C. They discussed the possibility of a photo-induced SC–M transition on the basis of their observation and suggested that such a photo-induced SC–M transition would be caused by the photo-induced bond breaking in Se helical chains. In this connection it should be noted that Sakaguchi and Tamura [18] measured the transient absorption spectra of liquid sulphur after illumination with a pulsed laser and that they found polymerization occurring even below the polymerization temperature, which suggests the possibility of photo-induced bond breaking. In relation to this experiment, Shimojo *et al* [19] confirmed theoretically the possibility of such a photo-induced bond breaking in an eight-membered ring of sulphur by means of first-principles molecular-dynamics simulation.

In this paper, we investigate the above-mentioned two types of SC–M transition, the 'temperature-induced' and the 'photo-induced' SC–M transitions, of liquid Se using first-principles MD simulation. The purposes of our first-principles MD simulation are as follows:

(i) to clarify how the SC–M transition at high temperatures and pressures is related to the structural change of liquid Se;

(ii) to investigate the possibility of inducing bond breaking in the Se chain by illumination with a pulsed laser; and

(iii) to discuss the microscopic mechanism of these SC–M transitions.

The method of calculation is described briefly in section 2. The results of our simulation at high temperatures and pressures are shown and discussed in section 3. Those for the isolated infinite Se chain are shown and discussed in section 4. Finally, section 5 summarizes our work.

2. The method of calculation

Our method of calculation is based on density functional theory, in which the generalized-gradient approximation [20] is used for the exchange–correlation energy. The wavefunctions are expanded in the plane-wave basis set and only the Γ point is used to sample the Brillouin zone of the supercell. For the electron–ion interaction we use the ultrasoft pseudopotential proposed by Vanderbilt [21]. The energy functional is minimized using an iterative scheme based on the preconditioned conjugate-gradient method [22–24] and the electronic charge density is obtained. Then the force acting on each ion is calculated using the Hellmann–Feynman theorem and the molecular-dynamics simulation is carried out using the force thus

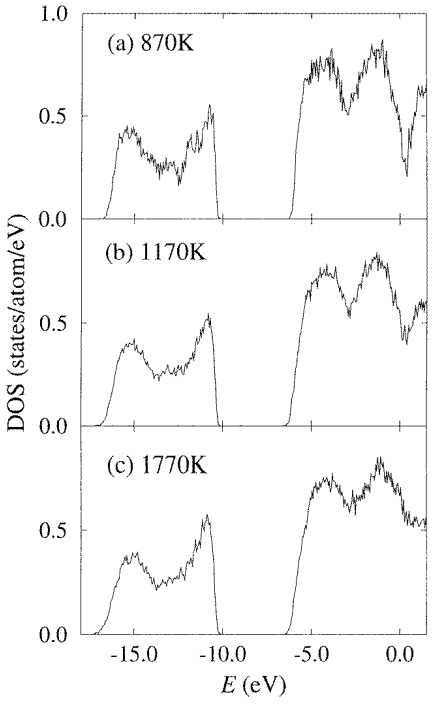

Figure 1. Electronic densities of states of fluid Se for (a) 870 K, (b) 1170 K and (c) 1770 K. The origin of energy ($E = 0$) is taken to be the Fermi level.

obtained to update the ionic configuration at the next time step. The equations of motion are solved via the velocity Verlet algorithm at a constant temperature using the Nosé–Hoover thermostat technique [25, 26].

The initial charge density at each MD step is estimated by extrapolating the charge densities at the previous steps [23], and the initial wavefunctions are estimated from the wavefunctions at the previous steps by a subspace diagonalization [27].

3. The semiconductor–metal transition at high temperatures and high pressures [16]

3.1. The model

We take 81 Se atoms in a cubic supercell with periodic boundary conditions. The simulations are carried out for three thermodynamic states with the following temperatures and densities: 870 K, 0.0286 Å^{-3}; 1170 K, 0.0270 Å^{-3}; 1770 K, 0.0254 Å^{-3}. These densities correspond to the supercell sizes $L = 14.15$, 14.42 and 14.72 Å, respectively, with L being a side of the supercell. These states are selected because x-ray diffraction measurements [8, 9] were carried out for the same conditions. The states at two temperatures, 870 and 1170 K, are in the semiconducting region, while the state at 1770 K is in the metallic region. The wavefunctions are expanded in the plane-wave basis set with a cut-off energy of 11 Ryd. In the MD simulation the time steps $\Delta t = 3.12$, 2.64 and 2.16 fs are used for the states at 870, 1170 and 1770 K, respectively. Each simulation is carried out for at least 4.5 ps. The quantities of interest are obtained by averaging over about 3 ps after the initial equilibration run of about 1.5 ps.

3.2. The electronic density of states

Figure 1 shows the temperature dependence of the electronic density of states (DOS), which is obtained from a time average of the distribution of the single-electron eigenvalues. The electronic states between −17 and −10 eV are s-like in character, those between −7 and −3 eV are p-like bonding states, those between −3 and 0 eV are p-like non-bonding states and those above 0 eV are p-like anti-bonding states. There is a dip at E_F in the DOS instead of a gap, because of taking the time average. We can, however, see a gap when the DOS is calculated for a fixed atomic configuration. In this case, the width and the position of the gap depend on the time. On the other hand, at 1770 K, the dip at E_F disappears, and there is no distinction between the p-like non-bonding and the p-like anti-bonding states. Thus, we have succeeded in reproducing the SC–M transition in fluid Se by means of our first-principles MD simulations.

3.3. Pair distribution functions

It is interesting to see how the structure of liquid Se changes with the SC–M transition. In figure 2 we show the pair distribution functions (PDFs) $g(r)$ (bold solid line) obtained by means of our simulation for three temperatures, 870, 1170 and 1770 K. The calculated $g(r)$ are in reasonable agreement with the experimental results due to Tamura and co-workers [8, 9]. It is seen, from figure 2, that the first peak of $g(r)$ is sharp, even at 1770 K, which means that the chain-like structure persists in the metallic state. However, the first

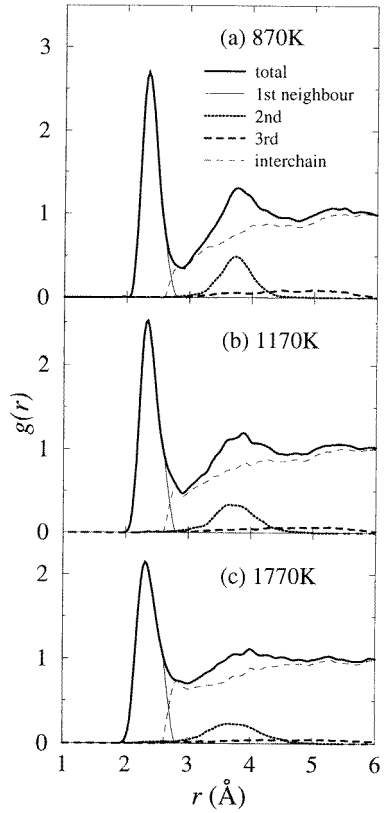

Figure 2. The pair distribution functions $g(r)$ (bold solid line) as well as interchain and intrachain pair distribution functions of fluid Se calculated at (a) 870 K, (b) 1170 K and (c) 1770 K. The thin solid, bold dotted and bold dashed lines show the first-neighbour, the second-neighbour and the third-neighbour intrachain pair distribution functions, respectively. The thin dashed line shows the interchain pair distribution function.

peak becomes lower and the first minimum becomes shallower with increasing temperature, which means that the chain structure is more disrupted at higher temperatures. The position r_1 of the first peak of $g(r)$ moves slightly to smaller r. The values of r_1 are 2.35, 2.34 and 2.32 Å at 870, 1170 and 1770 K, respectively. Note that these average nearest-neighbour distances are a little smaller than the distance found in trigonal Se, 2.37 Å. The coordination number N_1, which is estimated by the formula

$$2\rho \int_0^{r_1} 4\pi r^2 g(r)\ \mathrm{d}r$$

(with ρ being the number density of atoms), decreases slightly, which means that the average chain length decreases as the temperature increases. The values of N_1 are 1.9, 1.7 and 1.5 at 870, 1170 and 1770 K, respectively.

To investigate more closely how the chain structure changes with increasing temperature, we decompose the system into an assembly of twofold-coordinated chains. In order to do this, we decide whether two Se atoms belong to the same chain or not simply by considering the distance between them. If the distance between the two Se atoms is smaller than 2.7 Å, the position of the first minimum of $g(r)$, we consider that they belong to the same chain, and otherwise that they do not. In figure 2, we show the first-neighbour (thin solid line), the second-neighbour (bold dotted line) and the third-neighbour (bold dashed line) intrachain PDFs as well as the interchain PDF (thin dashed line). It is found that the second-neighbour intrachain PDF together with the interchain PDF contribute to form the second peak of $g(r)$, and the second peak becomes broader with increasing temperature. The third-neighbour intrachain PDF is very broad at any temperature. The first minimum of $g(r)$ is determined mainly by the interchain PDF, and becomes shallow at 1770 K. For these reasons the first minimum of $g(r)$ can be considered as a measure of how much the chain structure is disrupted. Note that the first minimum of $g(r)$ is zero and the first peak is separated from the second peak for liquid Se near the melting temperature, where liquid Se is composed of many long chains with about 10^5 atoms each.

3.4. Bond breaking and rearrangement of selenium chains

It is known experimentally that the average chain length decreases rapidly with increasing temperature and pressure, and approaches a value of only about 10 atoms in the metallic region [3]. From the chain-length distribution function $L(N)$, with N being the number of atoms per chain, obtained by our calculation, it is seen that, at 870 K, $L(N)$ is distributed over a wide range of N up to $N = 30$, while, at 1770 K, $L(N)$ is distributed mainly over small $N < 10$. This temperature dependence of $L(N)$ is in agreement with the experimentally observed tendency. By investigating the time change of the chain structure, it is found that the interaction between the Se chains is important for bond breaking and rearrangement of Se chains. When a Se chain moves in very close to one of the other chains, more than two Se atoms interact with each other, i.e. threefold coordinations are formed transiently. Since such threefold coordinations are unstable, bond breaking and rearrangement of the Se chains occur and, as a result, twofold-coordinated chains are formed. As a typical example of bond breaking and rearrangement of the Se chains, we show in figure 3 the time evolution of the local chain structure which is a part of the atomic configuration obtained from the MD simulation at 1770 K. In the figure, two Se atoms, whose distance apart is smaller than 2.7 Å, are connected by the bond. At 0 fs, the closest distance between the two Se chains is about 3.4 Å and, therefore, the two Se chains are considered to be well separated. However, these two chains approach each other in a short

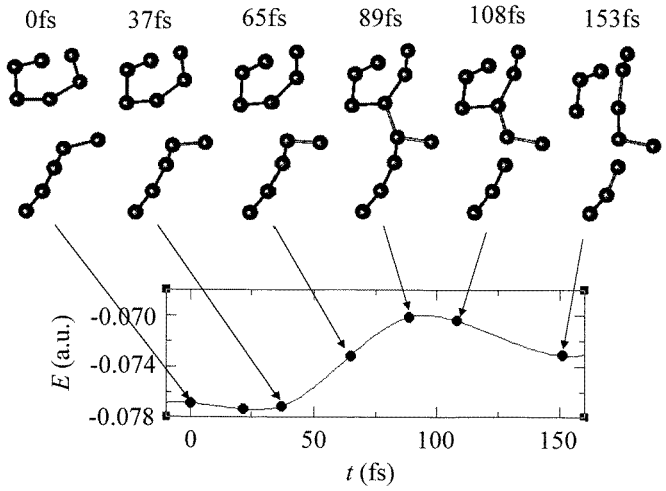

Figure 3. The time evolution of the local chain structure which is a part of the atomic configuration obtained by means of our MD simulation at 1770 K. Two Se atoms, whose distance apart is smaller than 2.7 Å, are connected by the bond. The energies of the corresponding configurations are also shown.

time, and at 89 fs a new bond is formed between them with threefold coordinations. It is seen that a Se atom is detached from the threefold-coordinated Se atom at 108 fs. At 153 fs, bond breaking occurs again, and finally three chains are formed without threefold coordination. To examine this rearrangement process of chains from the energetical point of view, we calculated the energies of the corresponding local configurations, which are also shown in figure 3. It is clearly seen that the threefold coordination is energetically unfavourable and the rearrangement of chains occurs so as to reduce the energy of the system. From such a careful and detailed investigation of the time change of the chain structure, we can see that bond breaking and rearrangement of Se chains take place almost always with the interaction between Se chains, and that the bond breaking in a single chain with no interaction with other chains hardly ever occurs. The probability that a Se chain contacts another chain becomes high due to the thermal motion of the atoms with increasing temperature. As a result, at high temperatures, bond breaking occurs frequently, and the average chain length decreases as mentioned above.

3.5. The mechanism of the semiconductor–metal transition

As discussed in the previous subsections, the helical chain structure persists in fluid Se even in the metallic state, though the average chain length decreases with increasing temperature. To display the microscopic origin of the appearance of the metallic state, we show in figure 4 the wavefunctions of those states with eigenenergies in the vicinity of the E_F. It is seen from this figure that these wavefunctions have large amplitudes near their ends. Therefore when the temperature is increased at a pressure of about 1 kbar, the length of the chains decreases and the number of chains increases, and as a result many ends of chains are produced. Since those states with large amplitudes of the wavefunctions near the ends of their chains have eigenenergies in the vicinity of E_F, there are very many eigenstates which fill up the energy gap of liquid Se.

It should be noted again that the electronic states below E_F are p-like bonding or

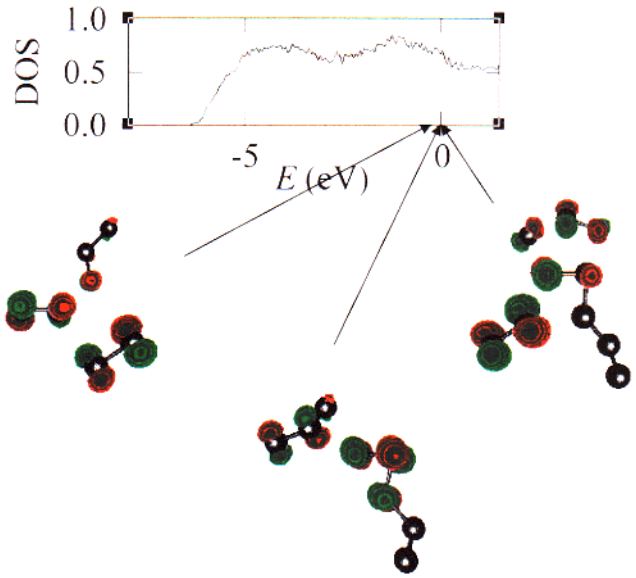

Figure 4. The wavefunctions of those states with eigenenergies in the vicinity of the Fermi level E_F, which is taken to be the origin of energy. The signs of the wavefunctions are shown by the different colours.

non-bonding in character, and those states above E_F are p-like anti-bonding in character. Recently, we have investigated the microscopic mechanism of bond breaking in the S_8 ring by means of first-principles molecular-dynamics simulation [19], and it was found that if bond breaking occurs, the anti-bonding states are stabilized, while the bonding or the non-bonding states become unstable. In the case of Se chains, we can also expect a similar phenomenon, as is shown below. If a chain is cut and the distance between the two Se atoms increases, the electronic states which have bonding or non-bonding character become unstable, while the electronic states which have anti-bonding character become stable. The structural changes described above indicate that such a situation occurs in fluid Se at high temperatures. It is considered that this is one of the elemental processes of the SC–M transition in fluid Se.

4. The photo-induced semiconductor–metal transition

4.1. The model

We take a Se helical chain composed of 14 atoms with 3.5-fold screw-rotation symmetry in a rectangular-parallelepiped cell, with the lengths of three sides being 12.0, 12.0 and 22.2 Å, and periodic boundary conditions are imposed for the three directions. Since the neighbouring chains are well separated, the model system can be considered as an assembly of isolated infinite chains. We employ the first-principles MD method described in section 2. About 7600 plane waves are used to expand the wavefunction. The simulation was carried out at the temperature of 500 K with a time step of 2.4 fs.

4.2. Photo-induced bond breaking

First, we performed our first-principles MD simulation of the infinite Se chain for 1 ps, in which we used as an initial configuration the ground-state geometry; the bond length is 2.34 Å, the bond angle is 110° and the dihedral angle is 81°. When a photon is absorbed

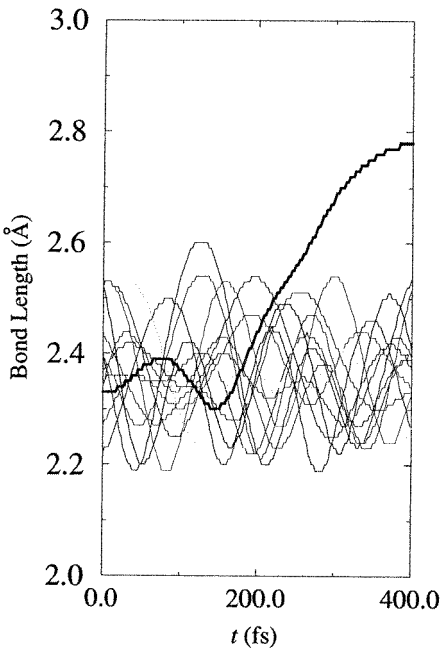

Figure 5. The time dependence of the Se–Se bond lengths of the selenium chain. The bond lengths for 14 Se–Se bonds are shown. The origin of time is the instant at which an electron in the HOMO is excited to the LUMO.

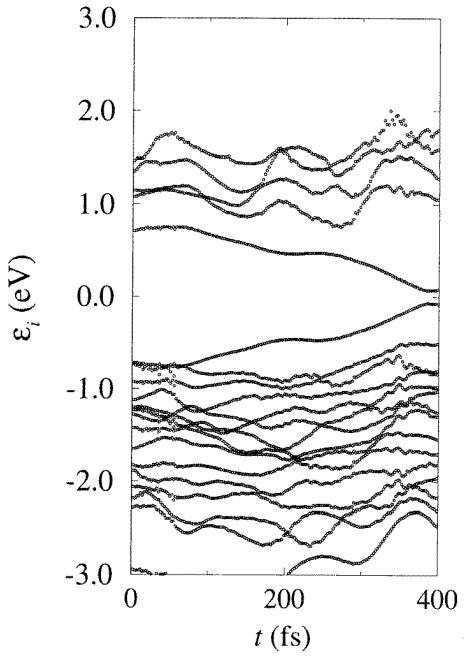

Figure 6. The time dependence of the energy eigenvalues. The origin of time is the same as that in figure 5.

by the infinite Se chain, an electron is excited to one of unoccupied states. To investigate the structural change of the Se chain due to the illumination by a pulsed laser, we carried out first-principles MD simulation of an infinite isolated chain by exciting an electron in the HOMO (highest occupied molecular orbital) to the LUMO (lowest unoccupied molecular orbital) at a certain MD step, and after that the electron configuration was fixed. In figure 5 we show the time dependence of the 14 Se–Se bond lengths of the Se chain in the MD cell. The origin of time is chosen to be the instant at which an electron in the HOMO is excited to the LUMO. For convenience we continue to use the terms 'HOMO' and 'LUMO' after the electron is excited, though they do not have their literal meanings any more. It is seen from figure 5 that, after the excitation, where the LUMO and the HOMO are each occupied by one electron, one of the bond lengths starts to increase suddenly at $t \simeq 200$ fs. Since, at $t \simeq 300$ fs, the bond length exceeds 2.7 Å, which is the position of the first minimum of $g(r)$ for liquid Se and is a possible longest bond length, the bond is considered to be broken.

4.3. The photo-induced change in the electronic states

In figure 6 we show the time dependence of the single-electron energy eigenvalues ε_i. Before an electron is excited, there is a gap of about 1.5 eV between the HOMO and the LUMO, which are characterized mainly as the non-bonding (lone-pair) 4p state and the anti-bonding 4p state, respectively. After the electron is excited, the eigenvalue of the

HOMO starts to increase, while that of the LUMO starts to decrease. Since the LUMO is the anti-bonding state, it is energetically favourable to release the high energy due to the electron occupation of the LUMO by breaking the bond.

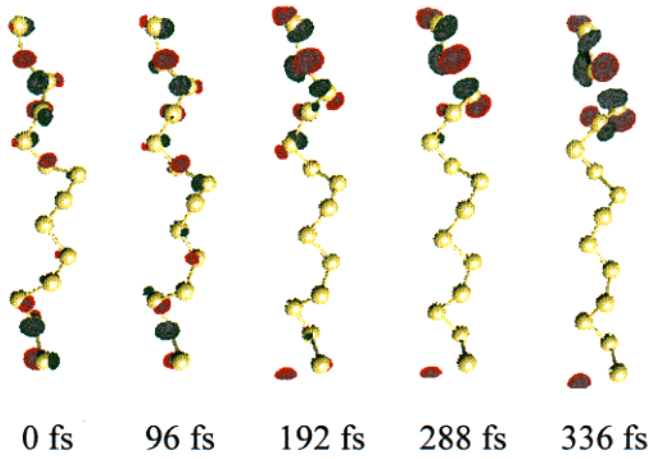

Figure 7. The time dependence of the wavefunctions of the LUMO. The origin of time is the same as that in figure 5. The signs of the wavefunctions are shown by the different colours.

To display this feature more clearly, we show in figure 7 the time dependence of the wavefunction of the LUMO, where the origin of time is the same as that in figure 5. At $t = 0$ fs, the wavefunction spreads over the whole chain and has an anti-bonding character, though the wavefunction is distorted from that of the ground state by the dynamics of the ions. After an electron is excited to the LUMO, the distribution of the wavefunction starts to change; i.e. the amplitude of the wavefunction increases around the Se–Se bond which will be broken, and decreases around other Se–Se bonds of the Se chain. At the same time the amplitude of the wavefunction of the HOMO is changed in a similar way to that of the LUMO. From these facts it is concluded that, when an electron is excited from the HOMO to the LUMO, one of the Se–Se bonds breaks so as to stabilize the anti-bonding LUMO state. As a result of the bond breaking, there appear states which have energy eigenvalues between the original HOMO and LUMO states, i.e. in the middle of the gap, whose wavefunctions have large amplitudes near both ends of the chains.

This bond-breaking phenomenon can be considered as one of the elemental processes of the photo-induced SC–M transition due to the illumination with the pulsed laser [17]. Since real liquid Se near the triple point is an assembly of long helical Se chains, the laser illumination may produce many shorter chains which have energy eigenvalues in the middle of the gap and have wavefunctions with large amplitude near their ends. As a result of these, the gap of the electronic density of states disappears and the system becomes metallic.

5. Summary

In this paper, we have investigated two types of semiconductor–metal transition, i.e. the 'temperature-induced' and the 'photo-induced' SC–M transitions, of liquid selenium using first-principles MD simulation. It is shown that, in both types of SC–M transition, the structural change of the Se chains is crucially important in the sense that there must exist many short chains in the metallic state because the eigenstates which fill up the energy gap of liquid Se and have large amplitudes of their wavefunctions near the ends of Se chains are produced by bond breaking. In the temperature-induced SC–M transition at high pressures, the interchain interactions and the thermal motions of Se chains result in rearrangement of

Se chains and production of many short chains. On the other hand, in the photo-induced SC–M transition, the excitation of an electron in the HOMO to the LUMO results in bond breaking in Se chains. In both cases there exists a common feature, i.e. when the Se–Se bonds break, the anti-bonding states above E_F are stabilized while the non-bonding states below E_F become unstable and as a result the gap disappears.

Acknowledgments

This work was supported by Grant-in-Aids for Scientific Research (No 07236102, No 08304026 and No 10640370) from the Ministry of Education, Science, Sports and Culture, Japan. We are grateful to Professor K Tamura, Professor M Watabe, Professor M Inui and Dr Y Sakaguchi for useful discussions and to Mr T Nishida for his help with the numerical calculations. We acknowledge the Computer Centre of the Institute for Molecular Science, Okazaki National Research Institute, Japan, for the use of the NEC SX-3/34R supercomputer.

References

[1] Perron J C, Rabit J and Rialland J F 1982 *Phil. Mag.* B **46** 321
[2] Freyland W and Cutler M 1980 *J. Chem. Soc. Faraday Trans.* **76** 756
[3] Warren W W Jr and Dupree R 1980 *Phys. Rev.* B **22** 2257
[4] Hoshino H, Schmutzler R W and Hensel F 1976 *Ber. Bunsenges. Phys. Chem.* **80** 27
[5] Hoshino H, Schmutzler R W, Warren W W Jr and Hensel F 1976 *Phil. Mag.* B **33** 255
[6] Edeling M and Freyland W 1981 *Ber. Bunsenges. Phys. Chem.* **85** 1049
[7] Tamura K and Hosokawa S 1992 *Ber. Bunsenges. Phys. Chem.* **96** 681
[8] Tamura K 1996 *J. Non-Cryst. Solids* **205–207** 239
[9] Inui M, Noda T and Tamura K 1996 *J. Non-Cryst. Solids* **205–207** 261
[10] Endo H 1983 *J. Non-Cryst. Solids* **59+60** 1047
[11] Hohl D and Jones R O 1991 *Phys. Rev.* B **43** 3856
[12] Kirchhoff F, Gillan M J and Holender J M 1996 *J. Non-Cryst. Solids* **205–207** 924
[13] Kirchhoff F, Gillan M J, Holender J M, Kresse G and Hafner J 1996 *J. Phys.: Condens. Matter* **8** 9353
[14] Almarza N G, Enciso E and Bermejo F J 1993 *J. Chem. Phys.* **99** 6876
[15] Bichara C, Pellegatti A and Gaspard J-P 1994 *Phys. Rev.* B **49** 6581
[16] Shimojo F, Hoshino K, Watabe M and Zempo Y 1998 *J. Phys.: Condens. Matter* **10** 1199
[17] Sakaguchi Y and Tamura K 1998 *J. Phys.: Condens. Matter* **10** 2209
[18] Sakaguchi Y and Tamura K 1995 *J. Phys.: Condens. Matter* **7** 4787
[19] Shimojo F, Hoshino K and Zempo Y 1998 *J. Phys.: Condens. Matter* **10** L177
[20] Perdew J P 1991 *Electronic Structure of Solids '91* ed P Ziesche and H Eschrig (Berlin: Akademie)
[21] Vanderbilt D 1990 *Phys. Rev.* B **41** 7892
[22] Teter M P, Payne M C and Allan D C 1989 *Phys. Rev.* B **40** 12 255
[23] Kresse G and Hafner J 1994 *Phys. Rev.* B **49** 14 251
[24] Shimojo F, Zempo Y, Hoshino K and Watabe M 1995 *Phys. Rev.* B **52** 9320
[25] Nosé S 1984 *Mol. Phys.* **52** 255
[26] Hoover W G 1985 *Phys. Rev.* A **31** 1695
[27] Arias T A, Payne M C and Joannopoulos J D 1992 *Phys. Rev.* B **45** 1538